Layered Steered Space–Time-Spreading-Aided Generalized MC DS-CDMA

M. El-Hajjar, O. Alamri, R. G. Maunder, and L. Hanzo

***Abstract*—We present a novel trifunctional multiple-input–multiple-output (MIMO) scheme that intrinsically amalgamates space–time spreading (STS) to achieve a diversity gain and a Vertical Bell Labs layered space–time (V-BLAST) scheme to attain a multiplexing gain in the context of generalized multicarrier direct-sequence code-division multiple access (MC DS-CDMA), as well as beamforming. Furthermore, the proposed system employs both time- and frequency-domain spreading to increase the number of users, which is also combined with a user-grouping technique to reduce the effects of multiuser interference. Further system performance improvements can be attained by serially concatenating our proposed scheme with an outer code that is amalgamated with a unity-rate code for the sake of improving the achievable decoding convergence behavior of the proposed system, which is evaluated with the aid of extrinsic information transfer charts. We also propose a novel logarithmic likelihood ratio (LLR) postprocessing technique to improve the iteratively detected system's performance. Explicitly, the proposed system can attain a second-order spatial diversity gain and a frequency diversity gain of order V, where V is the number of subcarriers. Additionally, the proposed system attains a beamforming gain and a multiplexing gain that is twice that of a single-input–single-output system. Furthermore, after $I = 10$ decoding iterations and employing an interleaver depth of $D_{\rm int} = 160\,000$ bits, a time-domain spreading factor of $N_e = 4$, and $V = 4$ subcarriers, the overloaded system supporting $K = 8$ users requires an E_b/N_0 that is only about 0.45 dB higher than the single-user system.**

***Index Terms*—Beam-forming, beam-steering, extrinsic information transfer (EXIT) charts, generalized multicarrier code-division multiple access (MC-CDMA), iterative detection, near-capacity coding, space-time spreading, spatial multiplexing.**

I. Introduction

Information-theoretic studies [1] have shown that, in contrast to the logarithmic Shannon–Hartley law, multiple-input–multiple-output (MIMO) schemes linearly increase the systems' capacity with the number of transmit antennas. Hence, when the extra power is assigned to additional antennas, it may be argued that the capacity also linearly increases with the transmit power. Inspired by the philosophy of space–time block codes (STBCs) [2], [3], Hochwald *et al.* [4] proposed the transmit diversity concept known as space–time spreading (STS) [5] for the downlink (DL) of wideband code-division multiple access [6]. Wolniansky *et al.* [7] proposed the multilayer MIMO structure known as the Vertical Bell Labs layered space–time (V-BLAST) scheme, whose transceiver is capable of providing a tremendous increase in a specific user's effective bandwidth efficiency without the need for any increase in the transmitted power or in the system's bandwidth. Furthermore, Onggosanusi *et al.* [8] presented a transmission scheme referred to as double space–time transmit diversity (DSTTD), which consists of two STBC units at the transmitter that is equipped with four transmit antennas, whereas the receiver is equipped with two antennas. The decoding of DSTTD is based on the low-complexity independent linear decoding scheme that is presented in [9], rather than on the joint maximum-likelihood detection of all the four transmit symbols.

On the other hand, beamforming [10] constitutes an effective technique of reducing the multiple-access interference with the aid of angular selectivity, where the antenna gain is increased in the direction of the desired user, while reducing the gain toward the interfering users. Several attempts have been made to design hybrid MIMO schemes combining an STBC with beamforming [11], [12].

The novelty and rationale of this paper can be summarized as follows.

1) A system that intrinsically amalgamates STS, V-BLAST, beamforming, as well as generalized multicarrier direct-sequence code-division multiple access (MC DS-CDMA) is proposed. The system is characterized by the spatial diversity gain of the STS, the multiplexing gain of the V-BLAST, the frequency diversity gain of the generalized MC DS-CDMA, as well as the beamforming gain. The proposed system is referred to as layered steered STS (LSSTS) aided generalized MC DS-CDMA. In the generalized MC DS-CDMA scheme that is considered in this paper, the subcarrier frequencies are arranged in a way that guarantees that the same STS signal is spread to and, hence, transmitted by the specific V number of subcarriers having the maximum possible frequency separation so that they experience independent fading and achieve the maximum attainable frequency diversity.
2) In contrast to the STS scheme, where the number of users supported is equal to the spreading factor N_e of the time-domain (TD) spreading code used, the proposed LSSTS scheme combines TD spreading with frequency-domain (FD) spreading to allow $N_e \cdot V$ users to communicate simultaneously, where V is the number of subcarriers that are employed in the generalized MC DS-CDMA.
3) Invoking TD and FD spreading by the LSSTS-aided generalized MC DS-CDMA imposes multiuser interference (MUI), which can be minimized by employing a novel user-grouping technique described in Section II-C.
4) The proposed LSSTS scheme is combined with a unity-rate code (URC) and a recursive systematic convolutional (RSC) code, where iterative decoding is employed between the constituent channel decoder at the receiver, and extrinsic information transfer (EXIT) charts [13] are used to analyze the convergence behavior of the proposed iterative-detection-aided scheme.
5) A novel log-likelihood ratio (LLR) postprocessing technique is contrived for improving the iteratively detected systems' performance. In this paper, we provide an empirical formula for the postprocessing in the LSSTS design. However, the proposed postprocessing technique is a general idea that can be used for any iteratively detected system.
6) Explicitly, after $I = 10$ decoding iterations and employing an interleaver depth of $D_{\rm int} = 160\,000$ bits, a TD spreading factor of $N_e = 4$, and $V = 4$ subcarriers, the overloaded system supporting $K = 8$ users requires an E_b/N_0 of only about 0.45 dB higher than the single-user system.

The rest of this paper is organized as follows. In Section II, we present the encoding and decoding algorithms of the novel LSSTS-aided generalized MC DS-CDMA scheme using TD and FD spreading. Iterative detection of the proposed system is discussed in

Manuscript received July 24, 2008; revised February 4, 2009 and May 17, 2009. First published July 14, 2009; current version published February 19, 2010. This work was supported by the European Community under the Seventh Framework Program Grant agreement ICT OPTIMIX nINFSO-ICT-214625 and in part by Vodafone under the auspices of the Dorothy Hodgkin Postgraduate Award. The review of this paper was coordinated by J. Wu.

The authors are with the School of Electronics and Computer Science, University of Southampton, SO17 1BJ Southampton, U.K. (e-mail: lh@ecs.soton.ac.uk).

Digital Object Identifier 10.1109/TVT.2009.2027734

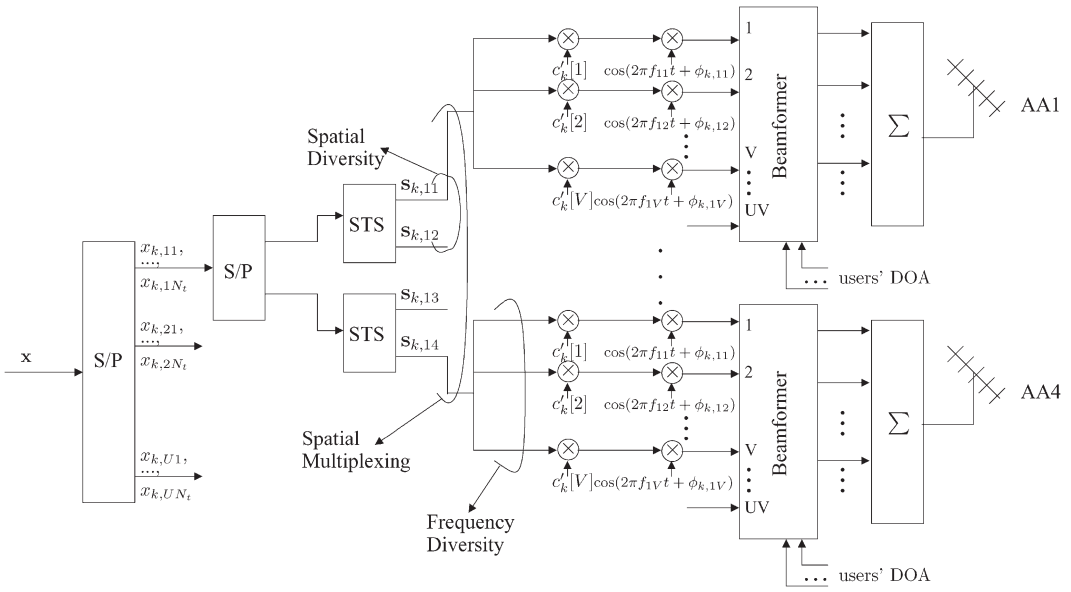

Fig. 1. kth user's LSSTS-aided generalized MC DS-CDMA transmitter model.

Section III, followed by a discussion of the attainable performance results in Section IV. Finally, we present our conclusions in Section V.

II. Layered Steered Space Time Spreading-Aided Generalized Multicarrier Direct-Sequence Code Division Miltiple Access

The system architecture employed in Fig. 1 for the proposed scheme is equipped with four transmit antenna arrays (AAs) that are sufficiently spaced far apart to experience independent fading. The $L_{\rm AA}$ number of elements of each of the AAs is spaced at a distance of half the wavelength for the sake of achieving beamforming. Furthermore, the receiver is equipped with two antennas. The system can support K users that are differentiated by their user-specific spreading code $\bar{\mathbf{c}}_k$, where $k \in [1, K]$. Additionally, in the generalized MC DS-CDMA considered, the subcarrier frequencies are arranged in a way that guarantees that each STS signal $\mathbf{s}_{k,un}$ of Fig. 1 is spread to and, hence, transmitted by the specific V number of subcarriers having the maximum possible frequency separation so that they experience independent fading and, hence, achieve the maximum attainable frequency diversity.

A. Transmitter Model

The system considered employs the generalized MC DS-CDMA scheme in [14] using UV number of subcarriers. The transmitter schematic of the kth user is shown in Fig. 1, where a block of $4U$ data symbols $\mathbf{x}$ is serial-to-parallel-converted (S/P-converted) to U parallel subblocks. Afterward, each set of four symbols is S/P-converted to $G = 2$ groups, where each group is encoded using the twin-antenna-aided STS procedure in [4].[1] The data are first S/P-converted to U subblocks, where each of the U parallel subblocks is encoded using a different set of V subcarriers. Additionally, each U subblock is S/P-converted into two groups, which are transmitted using the same V subcarriers from two STS blocks. The transmitted signal is spread to two transmit antennas with the aid of the orthogonal spreading codes of $\{\bar{\mathbf{c}}_{k,1}, \bar{\mathbf{c}}_{k,2}\}$, $k = 1, 2, \ldots, K$. The spreading codes $\bar{\mathbf{c}}_{k,1}$ and $\bar{\mathbf{c}}_{k,2}$ are generated from the same user-specific spreading code $\bar{\mathbf{c}}_k$ as in [4]. The discrete symbol duration of the orthogonal STS codes is $2 \cdot N_e$, where N_e represents the kth user's TD spreading factor.

The outputs of the STS blocks modulate a group of subcarrier frequencies $\{f_{u,1}, f_{u,2}, \ldots, f_{u,V}\}$. $\mathbf{c}' = [c'[1], c'[2], \ldots, c'[V]]$ shown in Fig. 1 is used in Section II-C to refer to the FD spreading code. Hence, in this section, where TD-only spreading is considered, $\mathbf{c}' = [1, 1, \ldots, 1]$ for all users. Since each of the U subblocks is spread to and, hence, conveyed with the aid of V subcarriers, a total of UV number of subcarriers are required in the generalized MC DS-CDMA system considered. The UV number of subcarrier signals are superimposed on each other to form the complex modulated signal. According to the kth user's channel information, the $4UV$ number of signals of the kth user are weighted by the transmit weight vector $\mathbf{w}_{uv,n}^{(k)}$ determined for his/her uvth subcarrier, which is generated for the nth AA. The kth user's signal transmitted from the ith transmit antenna, $i = 1, 2, 3,$ and 4 can be written as follows:

$$\mathbf{y}_{k,i} = \sum_{u=1}^{U} \sum_{v=1}^{V} \sqrt{\frac{2P_k}{VL_{AA}} \frac{1}{8}} \left(\mathbf{w}_{uv,i}^{k} \otimes I_{2N_e}\right) \cdot \mathbf{s}_{k,ui} \qquad (1)$$

where $\otimes$ represents the Hadamard product, P_k/V represents the transmitted power of each subcarrier, the factor L_{AA} in the denominator is due to beamforming, and the factor 8 in the denominator suggests that the STS scheme using four transmit antennas and two orthogonal spreading codes proportionally distributes its power in space and time. Assuming that the system employs a modulation scheme transmitting B bits/symbol, the resultant per-subcarrier bandwidth efficiency of the LSSTS-aided generalized MC DS-CDMA scheme is given by $2B$ bits/channel-use.

B. Receiver Model

The channel impulse response (CIR) vector $h_{uv,nm}$ spanning the nth transmit AA, $n \in [1, 4]$, and the mth receive antenna, $m \in [1, 2]$, while employing the uvth subcarrier can be expressed as

$$\mathbf{h}_{uv,nm}^{k} = \left[h_{uv,nm0}^{k}, h_{uv,nm1}^{k}, \ldots, h_{uv,nm(L_{AA}-1)}^{k}\right]^{T} \qquad (2)$$

[1] According to Fig. 1, after the two-stage S/P conversion, $s_{k,un} = x_{k,un}$, where $u \in [1, U]$ and $n \in [1, 4]$. In other words, $x_{k,11}$ and $x_{k,12}$ are transmitted from the first group of antennas and $x_{k,13}$ and $x_{k,14}$ from the second group.

where $h_{uv,nml}$ is the CIR with respect to the nmth link, the uvth subcarrier, and the lth element of the nth AA. Based on the assumption that the array elements are separated by half a wavelength, we can simplify $\mathbf{h}^k_{uv,nm}$ according to

$$\begin{aligned}\mathbf{h}^k_{uv,nm} &= \alpha^k_{uv,nm} \cdot \mathbf{d}^k_{nm} \\ &= \alpha^k_{uv,nm} \cdot \left[1, \exp\left(j\left[\pi \sin\left(\psi^k_{nm}\right)\right]\right), \ldots, \right. \\ &\qquad \left. \times \exp\left(j\left[(L_{AA}-1)\pi \sin\left(\psi^k_{nm}\right)\right]\right)\right]^T \quad (3)\end{aligned}$$

where $\alpha_{uv,nm}$ is a Rayleigh faded envelope, $\mathbf{d}^k_{nm} = [1, \exp(j[\pi \sin(\psi_{nm})]), \ldots, \exp(j[(L_{AA}-1)\pi \sin(\psi_{nm})])]^T$, and ψ_{nm} is the nmth link's direction of arrival (DOA). As for the AA specific DOA, we consider a scenario where the distance between the transmitter and the receiver is significantly higher than that between the AAs, and thus, we can assume that the signals arrive at the different AAs in parallel, i.e., the DOA at the different AAs is the same.

Assuming that K users' data expressed in the form of (1) are synchronously transmitted over a dispersive Rayleigh fading channel that is characterized by the CIR of (2), the complex-valued received signal of user 1 impinging on the mth receive antenna can be expressed as

$$\mathbf{z}^1_m = \sum_{k=1}^{K} \sum_{u=1}^{U} \sum_{v=1}^{V} \sum_{n=1}^{4} (\mathbf{h}_{uv,nm} \otimes I_{2N_e})^T \cdot \mathbf{y}_{k,uvn} + \mathbf{n}_m. \quad (4)$$

Let $\mathbf{w}^1_{uv,nm} = \mathbf{d}^{1\dagger}_{nm}$. Then, the $k = 1$st user's received signal matrix $\mathbf{r}$, including the received and despread data over the two receive antennas and the UV subcarriers after STS despreading, can be written as[2]

$$\mathbf{r} = \mathbf{H} \cdot \mathbf{X} + \mathbf{N} \quad (5)$$

where $\mathbf{H}$ and $\mathbf{X}$ can be arranged in a matrix form as in [9], and $\mathbf{N}$ represents the noise matrix. Detection is carried out in two steps: first, interference cancellation is performed according to the work in [8] and [9], followed by the STS decoding procedure in [4].

Finally, after combining the $k = 1$st user's identical replicas of the same signal transmitted by spreading over V number of subcarriers, the decision variables corresponding to the symbols transmitted in the uth subblock can be expressed as $\widetilde{x}_{1,u} = \sum_{v=1}^{V} \widetilde{x}_{1,uv}$. The decoded signal can be expressed as

$$\widetilde{x} = \sqrt{\frac{2P_1 L_{AA}}{V}} \frac{1}{8} \sum_{v=1}^{V} \left(|\widetilde{\alpha}_{uv,1}|^2 + |\widetilde{\alpha}_{uv,2}|^2\right) x + \eta. \quad (6)$$

Therefore, according to (6), the decoded signal has a diversity order of $2V$. More explicitly, second-order spatial diversity is attained from the STS operation, and a diversity order of V is achieved as a benefit of spreading by the generalized MC DS-CDMA scheme, where the subcarrier frequencies are arranged in a way that guarantees that the same STS signal is spread to and, hence, transmitted by the specific V number of subcarriers having the maximum possible frequency separation so that they experience near-independent fading.

We consider a system employing binary phase-shift keying modulation and a TD spreading factor of $N_e = 32$ for the sake of demonstrating the performance improvements achieved by the proposed LSSTS system. We assume the availability of perfect channel knowledge both at the receiver and at the beamformer. The resultant per-user per-subcarrier throughput is 2 bits/channel-use. Fig. 2 portrays the benefits of the individual components that are employed in the system, namely, those of the MC DS-CDMA, beamforming, STS, and

[2]In the following analysis, we remove the subscript uv for simplicity of notation.

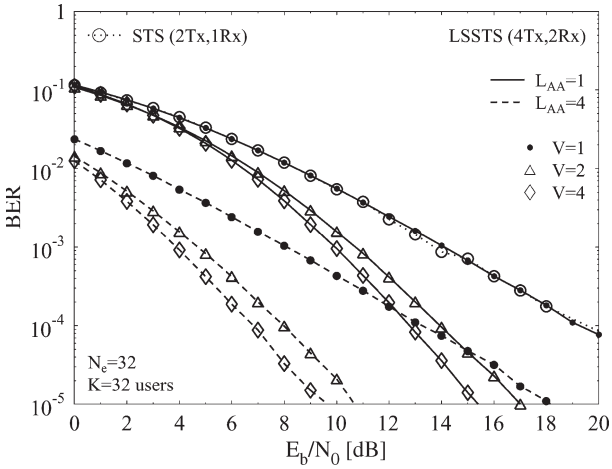

Fig. 2. BER performance of the LSSTS system in Fig. 1 employing four AAs and two antennas in conjunction with a varying number of L_{AA} elements per AA, as well as a varying number of subcarriers V, while supporting $K = 32$ users and employing a spreading factor $N_e = 32$. The per-user throughput is 2 bits/channel-use.

V-BLAST components. When a single carrier is employed, i.e., we have $V = 1$, and $L_{AA} = 1$ element per AA, the system's performance is identical to that of the STS scheme in [4]. Therefore, the system has a diversity order of two, whereas the bandwidth efficiency of the proposed system is twice that of the STS scheme in [4]. Additionally, Fig. 2 shows the beamforming gain that is achieved upon increasing the number of beam-steering elements L_{AA} in the AA, while maintaining the same total number of AAs. As shown in the figure, when the number of beam-steering elements L_{AA} increases, the achievable bit-error-rate (BER) performance substantially improves. Furthermore, to increase the achievable diversity order, the system employs $V > 1$ number of subcarriers, as shown in Fig. 2. Hence, the proposed system has a diversity order of $2V$ due to the employment of LSSTS-aided generalized MC DS-CDMA, and the throughput becomes twice that of a system employing only a single STS block, which is a benefit of the V-BLAST structure. Fig. 2 quantifies the advantages of increasing both L_{AA} and V in the proposed system, where increasing L_{AA} increases the signal-to-noise ratio gain of the system, whereas increasing V improves the attainable diversity order.

C. Increasing the Number of Users by Employing TD and FD Spreading

In the generalized MC DS-CDMA scheme considered, the transmitted data stream can be spread in the TD and the FD to support more users. When FD spreading is employed, after the STS-aided TD spreading stage of Fig. 1, FD spreading is applied by multiplying the data symbols of the V subcarriers with the V number of chip values of a spreading code that is invoked for spreading the data in the FD across the V number of subcarriers. Hence, the FD spreading factor is equal to V. The resultant bandwidth in this case is identical to that when TD-only spreading is considered.

When employing TD and FD spreading, the number of users supported by employing generalized MC DS-CDMA using both TD and FD spreading is equal to $N_e \cdot V$. In other words, the N_e users spread in the TD will have a unique spreading code in the FD, and the users having a different FD spreading code can share the same TD spreading code. The total number of users that are supported becomes $V \cdot \mathcal{K}_{\max} = V \cdot N_e$, which is V times the number of users that are supported by the scheme employing TD-only spreading.

Let us assume that the kth user's FD spreading code can be represented as $\bar{\mathbf{c}}'_k = \{c'_k[1], c'_k[2], \ldots, c'_k[V]\}$. The TD and FD orthogonal

spreading codes can be assigned as follows. If the number of users is still less than $\mathcal{K}_{\max}$, the users will be assigned with different TD spreading codes while sharing the same FD spreading code. The resultant scheme in this case is equivalent to that described in Section II-A. When the number of users is in the range of $v \cdot \mathcal{K}_{\max} \leq K \leq (v+1) \cdot \mathcal{K}_{\max}$, where $v = 1, 2, \ldots, V-1$, then the same TD orthogonal spreading code will be assigned to v users, where these users sharing the same TD code will be assigned with different FD orthogonal spreading codes. Hence, the users sharing the same TD spreading code can be distinguished by their corresponding FD spreading code. When employing TD and FD spreading, the kth user's transmitted signals can be expressed as

$$\mathbf{y}_{k,i} = \sum_{u=1}^{U} \sum_{v=1}^{V} \sqrt{\frac{2P_k}{VL_{AA}} \frac{1}{8}} \left(\mathbf{w}_{uv,i}^{k} \otimes I_{2N_e} \right) \cdot \mathbf{s}_{k,ui} \cdot c'_k[v]. \quad (7)$$

By employing the decoding scheme of Section II-B and after despreading the V number of decision variables with the aid of the V-chip FD spreading code $\bar{\mathbf{c}}'$, we arrive at

$$\widetilde{x} = \sqrt{\frac{2P_1}{VL_{AA}} \frac{1}{8}} \left[L_{AA} \sum_{v=1}^{V} \left(|\widetilde{\alpha}_{uv,1}|^2 + |\widetilde{\alpha}_{uv,2}|^2 \right) x + \bar{\mathbf{c}}'_1 \mathbf{i} \right] + \eta \quad (8)$$

where $\mathbf{i}$ represents a V-dimensional interference vector, and η represents the noise term after STS demodulation and FD despreading.

We observe from (8) that MUI is inevitably introduced since the orthogonality of the FD spreading codes cannot be retained for transmission over frequency-selective fading channels. Observe that the desired user's signal is not interfered with by the signals of the users that are employing different orthogonal TD spreading codes when assuming synchronous DL transmission, as well as flat fading of the individual subcarriers. The users sharing the same TD spreading code and employing different FD spreading codes interfere with each other. Therefore, we employ the user-grouping technique in [15] to minimize the associated FD interference.

In Fig. 3, we plot the BER performance of the proposed DL LSSTS-aided generalized MC DS-CDMA system using $V = 4$ subcarriers, $L_{AA} = 4$ elements per AA, and a TD spreading factor $N_e = 32$ for $K = 1$, 32, and 64 users. We assume having perfect channel knowledge at the receiver and the beamformer. As shown in Fig. 3, the performance of the system supporting $K = 32$ users is identical to that of the system serving a single user. This is due to the fact that there is no interference encountered by the $K = 32$ users since they employ different 32-chip orthogonal codes. On the other hand, for the sake of supporting $K = 64$ users, TD and FD spreading is used, where MUI is inevitably introduced among the users sharing the same TD spreading code. Fig. 3 shows that, for the case of $K = 64$ users, when no user grouping was employed, the BER performance of the system supporting $K = 64$ users was significantly worse than that supporting a single or even $K = 32$ users. However, when user grouping was employed by the LSSTS system for the sake of reducing the MUI imposed, the performance of the system supporting $K = 64$ users substantially improved.

Therefore, the LSSTS scheme can combine the benefits of STS, V-BLAST, and beamforming with the generalized MC DS-CDMA. The LSSTS decoder employs a two-stage detection technique, where interference cancellation is applied first to eliminate the interference that is imposed by the two STS layers on each other. Then, the decoding procedure of the STS scheme [4] is applied to the received signal after interference cancellation. Hence, the implementational complexity of the LSSTS scheme is almost equivalent to the combined

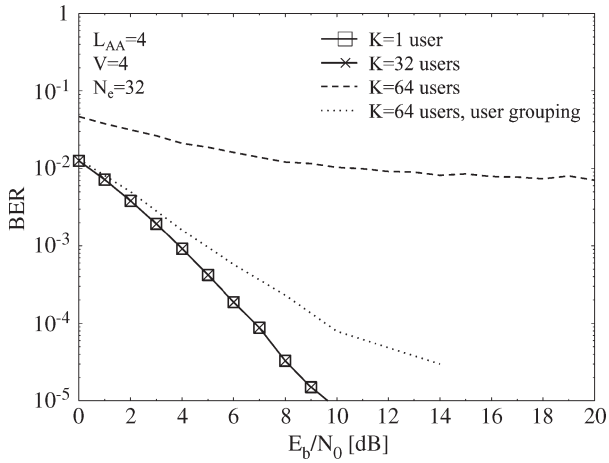

Fig. 3. BER performance of the proposed system in conjunction with a varying number of users, where both TD and FD spreading, as well as user grouping, were employed to improve the achievable system performance, while suppressing the MUI. The per-user throughput is 2 bits/channel-use.

complexities of the STS and V-BLAST decoders. The beamforming employed in the LSSTS scheme does not add much complexity to the decoder since the beamformer is employed at the transmitter, and hence, the decoder might be required to estimate the DOA, or the transmitter can estimate the DOA from the reverse channel. In the MC DS-CDMA, the receiver can apply serial processing, where one processor can successively decode the different subcarrier signals, or the different subcarrier signals can be simultaneously decoded using parallel processors. Additionally, the proposed scheme combines TD and FD spreading to increase the number of users that are supported from N_e to $V \cdot N_e$ users. The LSSTS decoder that is employed is less complex than applying an STS decoder supporting $V \cdot N_e$ users, where the different users are distinguished by a TD spreading code having a $V \cdot N_e$ spreading factor.

III. Iterative Detection and Exit Chart Analysis

Here, we design a quadrature phase shift keying (QPSK)-assisted LSSTS-aided generalized MC DS-CDMA system invoking iterative detection of serially concatenated RSC codes and URCs. In the proposed system seen in Fig. 4, the transmitted source bits are encoded by the outer RSC code's Encoder I. After RSC encoding, the coded bits are interleaved and then encoded by a URC encoder, followed by another interleaver, and then, they are transmitted using our QPSK-aided LSSTS scheme.

As shown in Fig. 4, the received and decoded complex-valued symbol stream $\tilde{\mathbf{x}}$ is fed into the QPSK demapper. The output of the demapper represents the LLR metric $L_M(\mathbf{b})$ passed from the QPSK demapper to the URC decoder. As seen in Fig. 4, the URC decoder processes the information that is forwarded by the demapper in conjunction with the *a priori* information that is passed from the outer RSC decoder to generate the *a posteriori* probability. The *a priori* LLR values of the URC decoder are subtracted from the *a posteriori* LLR values to generate the extrinsic LLR values $L_{II,e}(\mathbf{u}_2)$, and then, the LLRs $L_{II,e}(\mathbf{u}_2)$ are deinterleaved by a soft-bit deinterleaver, as seen in Fig. 4. Next, the soft bits $L_{I,a}(\mathbf{c}_1)$ are passed to the RSC decoder of Fig. 4 to compute the *a posteriori* LLR values $L_{II,p}(\mathbf{c}_1)$ for all the channel-coded bits $\mathbf{c}_1$. During the last iteration, only the LLR values $L_{I,p}(\mathbf{u}_1)$ of the original uncoded systematic information bits are required, which are passed to the hard decision decoder of Fig. 4 to determine the estimated transmitted source bits. As seen in Fig. 4, the extrinsic information $L_{I,e}(\mathbf{c}_1)$ is fed back to the URC decoder

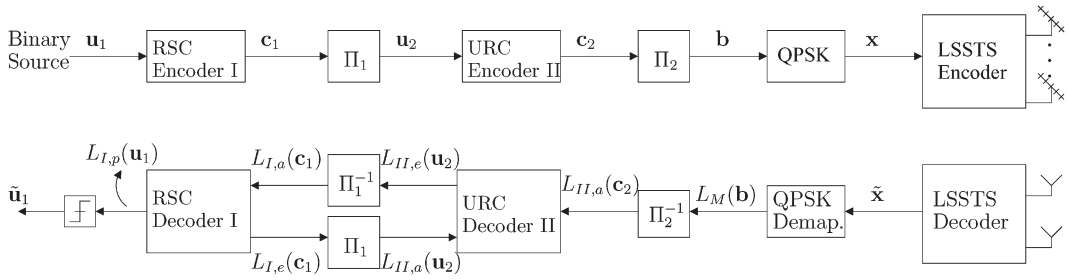

Fig. 4. Block diagram of the proposed DL iteratively detected system employing an RSC encoder in series with a URC encoder and transmitting through a QPSK-aided LSSTS.

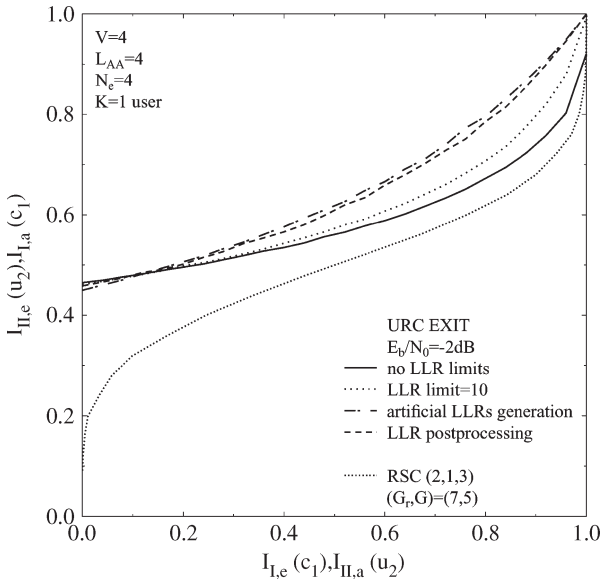

Fig. 5. Extrinsic information transfer function of an RSC-coded and URC-precoded proposed iteratively detected system of Fig. 4 employing GM-aided QPSK in conjunction with 4, 2, $V = 4$, $L_{AA} = 4$, $K = 1$ user, and $E_b/N_0 = -2$ dB.

as the *a priori* information $L_{I,a}(\mathbf{u}_2)$ after appropriately reordering them using the interleaver of Fig. 4. The URC decoder exploits the *a priori* information for the sake of providing improved *a posteriori* LLR values, which are then passed to the one-half-rate RSC decoder and then back to the URC decoder for further iterations.

A. EXIT Charts and LLR Postprocessing

Fig. 5 shows the extrinsic information transfer function of the iteratively detected system depicted in Fig. 4. The system employs a one-half-rate memory-2 RSC code, denoted as RSC(2, 1, 3), in conjunction with an octal generator polynomial of $(G_r, G) = (7, 5)_8$, where G_r is the feedback polynomial, and G is the feedforward polynomial. Encoder II is a simple URC scheme, described by the pair of octal generator polynomials $(G_r, G) = (3, 2)_8$. Furthermore, the extrinsic information transfer function of Fig. 5 was generated for the system employing four transmit AAs and two antennas while using $L_{AA} = 4$ elements per AA and $V = 4$ subcarriers.

Observe in Fig. 5 that there are several extrinsic information transfer function curves for the URC decoder for the same E_b/N_0 value. Let us first consider the dark line marked by the legend "no LLR limits." This extrinsic information transfer function corresponds to the URC decoder of Fig. 4, which has a recursive encoder at the transmitter, and, hence, it is expected that the extrinsic information transfer function of the URC decoder will, indeed, reach the (1.0, 1.0) point of perfect convergence in the EXIT curve, as discussed in [16]. However, Fig. 5 also shows that the extrinsic information transfer function of the URC decoder does not reach the (1.0, 1.0) point. As a first step in circumventing this problem, we attempted to limit the maximum and the minimum of the LLR values $L_M(\mathbf{b})$ for the sake of avoiding the problem of numerical overflow in the computer's memory. Limiting the LLR values allowed the URC extrinsic information transfer function to reach the (1.0, 1.0) point, as shown in Fig. 5 by the dotted line associated with the legend "LLR limit $= 10$." On the other hand, for the sake of testing the accuracy of the URC EXIT curve, while imposing a limit on the LLR values, we generated artificial Gaussian-distributed and uncorrelated LLRs $L_M(\mathbf{b})$ that satisfy the consistency condition[3] that is defined in [17]. The resultant extrinsic information transfer function is then represented by the dotted line having the legend "artificial LLR generation." The artificial LLRs are generated assuming that the transmitted bits are known at the receiver. As shown in Fig. 5, the curves corresponding to the case where the LLRs' dynamic range is limited and where the artificial LLRs are generated are quite different. Therefore, limiting the LLR values does not solve the problem.

The reason for this behavior is the fact that the input $\tilde{\mathbf{x}}$ of the QPSK demapper is not Gaussian distributed, although we calculate the LLR values $L_M(\mathbf{b})$, assuming that the input data stream $\tilde{\mathbf{x}}$ is Gaussian distributed. A trivial solution to this problem is to try and find the probability distribution of the LSSTS decoder's output $\tilde{\mathbf{x}}$ and compute the LLRs in the QPSK demapper using the correct probability density function (pdf). However, it is not straightforward to find a mathematical formula to model the pdf of $\tilde{\mathbf{x}}$. On the other hand, it is possible to compute the LLRs based on the histogram of the received and decoded data $\tilde{\mathbf{x}}$. However, computing the histogram for every received frame is a complex and time-consuming process.

An empirical transformation of the $L_M(\mathbf{b})$ LLR values has been found for correcting the relationship between the LLR values and their corresponding probabilities so that the LLR values satisfy the consistency condition in [17]. The transformation is applied to the LLR values at the output of the QPSK demapper, and hence, it is referred to as LLR postprocessing. The resultant empirical transformation can be expressed as

$$\mathrm{LLR}_{\mathrm{out}} = \frac{L_M(\mathbf{b})}{1.25\left(\log_2(V)+1\right) - 0.75\left\lceil \frac{K}{N_e} - 1 \right\rceil} \tag{9}$$

where $\mathrm{LLR}_{\mathrm{out}}$ represents the LLR passed from the QPSK demapper to the deinterleaver Π_2 of Fig. 4 after the transformation of the LLRs. Fig. 5 also shows the extrinsic information transfer function of the inner URC decoder after the LLR postprocessing technique was employed. As shown in Fig. 5, the extrinsic information transfer

[3]The consistency condition in [17] satisfies $p(-\zeta/d) = e^{-d\zeta}p(\zeta/d)$.

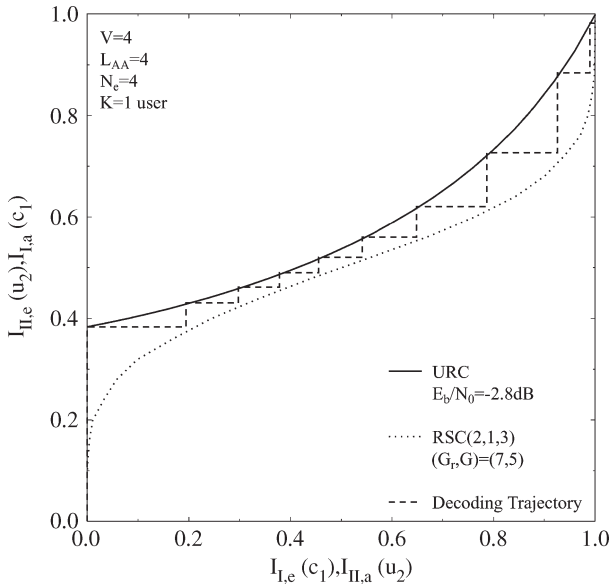

Fig. 6. Decoding the trajectory of the iteratively detected RSC-coded and URC-precoded LSSTS system seen in Fig. 4 employing an interleaver depth of $D_{\rm int} = 160\,000$ bits, $V = 4$ subcarriers, $L_{AA} = 4$ elements per AA, $N_e = 4$, and $K = 1$ user, while operating at $E_b/N_0 = -2.8$ dB.

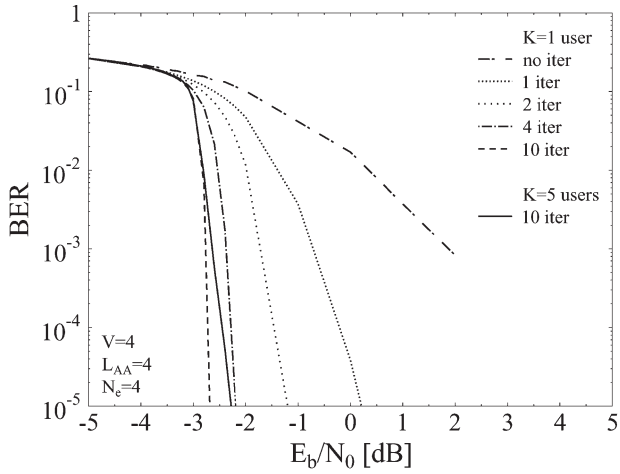

Fig. 7. Performance comparison of the GM-based RSC-coded and URC-precoded System 1 of Fig. 4 in conjunction with $V = 4$ subcarriers, $L_{AA} = 4$ elements per AA, $N_e = 4$, and $K = 1$ user, when using an interleaver depth of $D_{\rm int} = 160\,000$ bits for a variable number of iterations.

function of the system where the LLR postprocessing is employed is similar to that where the artificial LLRs were considered.

The EXIT-chart-based convergence predictions can be verified by the Monte Carlo-simulation-based iterative decoding trajectory of Fig. 6, where the trajectory was recorded at $E_b/N_0 = -2.8$ dB, while using an interleaver depth of $D_{\rm int} = 160\,000$ bits, $V = 4$ subcarriers, $L_{AA} = 4$ elements per AA, $N_e = 4$, and $K = 1$ user.

IV. Results and Discussions

Here, we consider an LSSTS system that is associated with four transmit AAs, two receive antennas, $V = 4$ subcarriers, $L_{AA} = 4$ elements per AA, and $N_e = 4$. Additionally, perfect channel knowledge is assumed at the receiver and the transmit beamformer.

Fig. 7 compares the BER performance of the proposed iteratively detected system supporting $K = 1$ user in conjunction with gray mapping (GM) aided QPSK for a different number of iterations when employing an interleaver depth of $D_{\rm int} = 160\,000$ bits. Fig. 7 demonstrates that the BER performance closely matches the EXIT-chart-based prediction of Fig. 6, where the system approaches a BER below 10^{-5} at $E_b/N_0 = -2.8$ dB after $I = 10$ iterations. On the other hand, Fig. 7 also compares the BER performance of the iterative-detection-aided system for $K = 1$ and $K = 8$ users. According to Fig. 7, when the system employs an interleaver depth of $D_{\rm int} = 160\,000$ bits and $I = 10$ decoding iterations, our overloaded $K = 8$ user system requires an E_b/N_0 of only about 0.45 dB at a BER of 10^{-5} higher than the single-user benchmark system.

V. Conclusion

In this paper, we have proposed a novel multifunctional DL MIMO scheme that intrinsically amalgamates STS, V-BLAST, generalized MC DS-CDMA, as well as beamforming. Additionally, to increase the number of users so that the system can support more than N_e number of users, where N_e is the TD spreading factor, TD and FD spreading has been employed. We have also employed a user-grouping technique for the sake of minimizing the multiuser interference that is imposed by the users sharing the same TD spreading code on each other. To improve the achievable performance of the proposed system, we have presented the iterative-detection-aided structure of Fig. 4 and proposed an LLR postprocessing technique to improve the attainable system performance. Explicitly, the proposed system can attain a second-order spatial diversity gain and a frequency diversity gain of order V, where V is the number of subcarriers. Additionally, the proposed system attains a beamforming gain and a multiplexing gain that is twice that of a single-input–single-output system. Furthermore, after $I = 10$ decoding iterations and employing an interleaver depth of $D_{\rm int} = 160,000$ bits, a TD spreading factor of $N_e = 4$, and $V = 4$ subcarriers, the overloaded system supporting $K = 8$ users requires an E_b/N_0 of only about 0.45 dB higher than the single-user system.

References

[1] G. J. Foschini and M. J. Gans, "On limits of wireless communications in a fading environment when using multiple antennas," *Wirel. Pers. Commun.*, vol. 6, no. 3, pp. 311–335, Mar. 1998.

[2] S. M. Alamouti, "A simple transmit diversity technique for wireless communications," *IEEE J. Sel. Areas Commun.*, vol. 16, no. 8, pp. 1451–1458, Oct. 1998.

[3] V. Tarokh, H. Jafarkhani, and A. R. Calderbank, "Space–time block codes from orthogonal designs," *IEEE Trans. Inf. Theory*, vol. 45, no. 5, pp. 1456–1467, Jul. 1999.

[4] B. Hochwald, T. L. Marzetta, and C. B. Papadias, "A transmitter diversity scheme for wideband CDMA systems based on space–time spreading," *IEEE J. Sel. Areas Commun.*, vol. 19, no. 1, pp. 48–60, Jan. 2001.

[5] L. Hanzo, O. Alamri, M. El-Hajjar, and N. Wu, *Near-Capacity Multi-Functional MIMO Systems: Sphere-Packing, Iterative Detection and Cooperation*. Piscataway, NJ: IEEE Press, 2009.

[6] L. Hanzo, L.-L. Yang, E.-L. Kuan, and K. Yen, *Single and Multi-Carrier DS-CDMA: Multi-User Detection, Space–Time Spreading, Synchronisation, Networking and Standards*. New York: IEEE Press, 2003.

[7] P. W. Wolniansky, G. J. Foschini, G. D. Golden, and R. A. Valenzuela, "V-BLAST: An architecture for realizing very high data rates over the rich-scattering wireless channel," in *Proc. Int. Symp. Signals, Syst., Electron.*, Pisa, Italy, Sep. 1998, pp. 295–300.

[8] E. N. Onggosanusi, A. G. Dabak, and T. A. Schmidl, "High rate space–time block coded scheme: Performance and improvement in correlated fading channels," in *Proc. IEEE WCNC*, Mar. 2002, vol. 1, pp. 194–199.

[9] A. F. Naguib, N. Seshadri, and A. R. Calderbank, "Increasing data rate over wireless channels," *IEEE Signal Process. Mag.*, vol. 17, no. 3, pp. 76–92, May 2000.

[10] L. Hanzo, J. Blogh, and S. Ni, *3G, HSPA and FDD Versus TDD Networking: Smart Antennas and Adaptive Modulation*, 2nd ed. New York: Wiley, Feb. 2008

[11] G. Jongren, M. Skoglund, and B. Ottersten, "Combining beamforming and orthogonal space–time block coding," *IEEE Trans. Inf. Theory*, vol. 48, no. 3, pp. 611–627, Mar. 2002.
[12] J. Liu and E. Gunawan, "Combining ideal beamforming and Alamouti space–time block codes," *Electron. Lett.*, vol. 39, no. 17, pp. 1258–1259, Aug. 2003.
[13] S. Ten Brink, "Designing iterative decoding schemes with the extrinsic information transfer chart," *AEÜ Int. J. Electron. Commun.*, vol. 54, no. 6, pp. 389–398, Nov. 2000.
[14] L.-L. Yang and L. Hanzo, "IPerformance of generalized multicarrier DS-CDMA over Nakagami-m fading channels," *IEEE Trans. Commun.*, vol. 50, no. 6, pp. 956–966, Jun. 2002.
[15] M. El-Hajjar, B. Hu, L.-L. Yang, and L. Hanzo, "Coherent and differential downlink space–time steering aided generalised multicarrier DS-CDMA," *IEEE Trans. Wireless Commun.*, vol. 6, no. 11, pp. 3857–3863, Nov. 2007.
[16] M. El-Hajjar, O. Alamri, S. X. Ng, and L. Hanzo, "Turbo detection of precoded sphere packing modulation using four transmit antennas for differential space–time spreading," *IEEE Trans. Wireless Commun.*, vol. 7, no. 3, pp. 943–952, Mar. 2008.
[17] J. Hagenauer, "The EXIT chart—Introduction to extrinsic information transfer in iterative processing," in *Proc. Eur. Signal Process. Conf.*, Vienna, Austria, Sep. 2004, pp. 1541–1548.

The Role of Phase Compensation in Preventing Channel Dispersion in Variable-Gain Relay OFDM Systems

Kyungchul Kwak, *Student Member, IEEE*,
Sungeun Lee, *Student Member, IEEE*, and
Daesik Hong, *Senior Member, IEEE*

***Abstract*—We show that the length of a composite channel is regarded up to the whole symbol duration for variable-gain relay (VGR), which generates the received power constant instantaneously. The enlarged channel length causes system burden, which is due to long-channel estimation, i.e., an increase in pilot overhead, a decrease in bandwidth efficiency, and a degradation of system performance. To prevent this effect and minimize the length of the composite channel, phase compensation of the source–relay (S–R) link channel should be added to the VGR, although this addition increases complexity. A system that adopts VGR with phase compensation performs better and has higher bandwidth efficiency.**

***Index Terms*—Amplify-and-forward (AF) relays, channel estimation, orthogonal frequency-division multiplexing (OFDM).**

I. Introduction

Wireless relay has recently attracted a great deal of attention as a way to increase capacity and link coverage [1], [2]. It is generally broken down into two categories: 1) amplify-and-forward (AF) relaying and 2) decode-and-forward (DF) relaying [2].

Manuscript received April 1, 2009; revised August 21, 2009. Current version published February 19, 2009. This work was supported in part by the Korea Science and Engineering Foundation through the National Research Laboratory Program under Grant R0A-2007-000-20043-0 and in part by the Ministry of Knowledge Economy, Korea, through the Information Technology Research Center support program supervised by the National IT Industry Promotion Agency under Grant NIPA-2009-(C1090-0902-0005). The review of this paper was coordinated by Prof. H. Liu.

K. Kwak and D. Hong are with the Department of Electrical and Electronic Engineering, Yonsei University, Seoul 120-749, Korea (e-mail: chulli@yonsei.ac.kr; daesikh@yonsei.ac.kr).

S. Lee is with the Department of Electrical and Computer Engineering, Georgia Institute of Technology, Atlanta, GA 30332 USA (e-mail: softmind@yonsei.ac.kr).

Digital Object Identifier 10.1109/TVT.2009.2035045

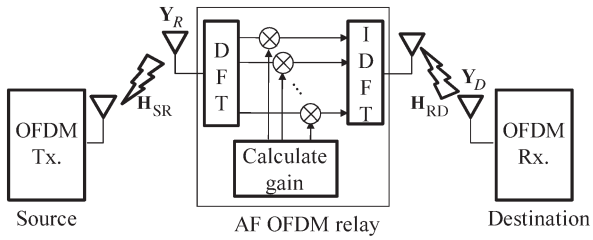

Fig. 1. Block diagram of the AF OFDM relay system.

With AF relay, the demodulation and equalization processes are only performed at the destination. Therefore, any investigation concerned with channel properties must look at both the source–relay (S–R) link and the relay–destination (R–D) link or the composite channel.

Patel *et al.* investigated time selectivity in the composite channel in an AF relay system [3]. They said that it is determined not only by the mobility of each node but also by the type of relay gain, e.g., variable-gain relay (VGR) or fixed-gain relay (FGR). VGR uses the instantaneous channel amplitude to generate the output power constant instantaneously. FGR exploits average power and noise to generate the output power constant statistically [2], [4].

However, not enough research has been conducted on frequency selectivity in the composite channel of AF relay systems [1]–[3], [5]. The statistics on composite channels in the frequency domain should be examined to use AF relay systems over the frequency-selective fading channel. The composite channel can be considered a convolution of three systems, namely, the S–R link channel, power scaling, and the R–D link channel, on the assumption that they are independent linear time-invariant systems. However, this explanation is only valid for FGR, and the frequency selectivity for VGR is quite different, since power scaling depends on the instantaneous channel amplitude.

We show that the length of the composite channel for VGR is greatly increased by analyzing the effective channel on the S–R link after power scaling. Since a longer channel generally degrades system performance in terms of pilot overhead, bandwidth efficiency, and error performance, the length of the composite channel should be minimized. Since power scaling is the only controllable factor for reducing the length among the three cascaded systems, we propose a new VGR scheme that compensates the relay for the residual phase in Section III. Simulation results in Section IV prove that the proposed method should be necessary for the orthogonal frequency-division multiplexing (OFDM) VGR system with a frequency-selective fading channel.

II. System Model

A. AF OFDM Relay System Model

Let us consider OFDM as the type of multiple access [6]. We assume that the destination cannot directly communicate with the source because of geometry or power consumption. In addition, without a loss of generality, it is assumed that the entire bandwidth is assigned to a single destination; this is because frequency allocation represents a different type of problem altogether and is beyond the scope of this paper. In addition, we assume that the synchronization of time and frequency is perfect.

Let us assume that the relay protocol is half-duplex [8], so that data transmission is performed at two time slots. The block diagram of the AF OFDM system is shown in Fig. 1. Then, based on the property